Separation Science and Technology
Publication details, including instructions for authors and subscription information:
http://www.informaworld.com/smpp/title~content=t713708471

Study of Nonlinear Wave Propagation Theory. II. Interference Phenomena of Single-Component Dye Adsorption Waves

Jia-Ming Chern[a]; Shi-Nian Huang[a]
[a] DEPARTMENT OF CHEMICAL ENGINEERING, TATUNG INSTITUTE OF TECHNOLOGY, TAIPEI 104, TAIWAN, REPUBLIC OF CHINA

Online publication date: 07 December 1999

To cite this Article Chern, Jia-Ming and Huang, Shi-Nian(1999) 'Study of Nonlinear Wave Propagation Theory. II. Interference Phenomena of Single-Component Dye Adsorption Waves', Separation Science and Technology, 34: 10, 1993 — 2011
To link to this Article: DOI: 10.1081/SS-100100751
URL: http://dx.doi.org/10.1081/SS-100100751

SEPARATION SCIENCE AND TECHNOLOGY, **34**(10), pp. 1993–2011, 1999

Study of Nonlinear Wave Propagation Theory. II. Interference Phenomena of Single-Component Dye Adsorption Waves

JIA-MING CHERN* and SHI-NIAN HUANG
DEPARTMENT OF CHEMICAL ENGINEERING
TATUNG INSTITUTE OF TECHNOLOGY
40 CHUNGSHAN NORTH ROAD, 3RD SEC., TAIPEI 104, TAIWAN, REPUBLIC OF CHINA

ABSTRACT

Yellow acid dye was adsorbed from aqueous solution by granular activated carbon packed in a column. The feed concentration was kept constant for a period of time and then switched to another level to simulate the concentration variation in wastewater treatment processes. The resulting breakthrough curves were experimentally measured and theoretically predicted. Explicit equations and an algorithm were developed based on the wave interference theory to predict the column breakthrough curves of single-component adsorption processes with step change in the feed concentration. The experimental results show that the wave interference theory predicts the column breakthrough curves satisfactorily.

Key Words. Wave propagation; Fixed-bed dynamics; Dye; Activated carbon; Adsorption; Wave interference

INTRODUCTION

Fixed-bed operations are widely used in chemical processes and pollution control processes such as separating ions by ion-exchange bed or removing toxic organic compounds by carbon adsorption bed. A powerful tool that can be used to predict fixed-bed column dynamics without tedious column tests and sophisticated mass-transfer modeling is the nonlinear wave propagation theory (1, 2). The concept of "wave" was first introduced by Klotz (3), and the

*To whom correspondence should be addressed. Telephone: 01188625925252 ext. 3487. FAX: 01188625861939. E-mail: JMCHERN@CHE.TTIT.EDU.TW

wave sharpening tendency, self-sharpening or nonsharpening, was first discussed by Glueckauf and Coates (4). Following these pioneer studies, the chromatography theory was successfully established and applied for chemical analysis and preparation purposes. The initiation of the "coherence" concept by Helfferich (5, 6) made a great contribution to the multicomponent chromatography theory. The development history of the nonlinear wave propagation theory can be found in two excellent review papers (7, 8). This paper is not meant to reinvent the chromatography theory, but to develop more explicit expressions from the theory to analyze the experimental breakthrough data of the activated carbon adsorption process with feed composition change.

The textile industry discharges wastewater with high color, high suspended solids, and dissolved organics. Due to its variation in pH, temperature, flow rate, and contained pollutants, textile wastewater usually requires physicochemical as well as biological treatments to meet the more stringent effluent standards. Besides chemical oxygen demand, color removal from textile wastewater is of primary concern. An effective method to remove color is to use an adsorbent such as activated carbon to adsorb the dye molecules and then remove the color from the wastewater (9–17). Although this direct addition of powdered activated carbon is quite efficient, the carbon loss as wasted sludge is rather significant. Granular activated carbon is usually used in the fixed-bed adsorption process because of ease of operation and no carbon loss problem. To design and operate a fixed-bed adsorption process successfully, the column dynamics must be understood; that is, the breakthrough and desorption curves under specific operating conditions must be predictable.

The design procedure for a fixed-bed process is quite straightforward and is well documented (18, 19). Using the nonlinear wave propagation theory, one can easily calculate the breakthrough volume for a specific feed concentration and design the fixed-bed volume with a proper choice of safety factor. However, the operating strategy of a fixed bed is rather complicated, especially when the feed concentration varies with operating time. Although the equalization tank in a wastewater treatment process can even the flow-rate variation, concentration variation is still inevitable. Therefore, the feed dye concentration to an activated carbon bed can vary with operating time. This variation of the feed concentration makes the column dynamics more complicated than the case of constant feed concentration.

In the language of wave propagation theory, the concentration wave velocity is defined as the variation of the traveling distance with time for a given concentration. Therefore, different concentrations possess different traveling velocities. If the traveling velocity for the first feed concentration is slower than that of the second feed concentration, then the first feed concentration will be caught by the second and this will result in wave interference phenomena. The general wave interference phenomena of multicomponent sys-

tems were examined in detail in a recent paper (20). This study focuses on applying the wave interference concept, developing more explicit expressions to predict the effluent histories of single-component adsorption systems, and verifying the predicted results with dye adsorption data.

WAVE INTERFERENCE THEORY

The theoretical basis of this study is directly built upon the nonlinear wave propagation theory developed by Helfferich and his coworkers (1, 20). Consider a carbon bed presaturated with a very low dye concentration, C_P. At time zero, a feed stream with dye concentration C_{F1} enters the bed at linear velocity u_0. After operating for a while at $t = t_0$, the feed dye concentration switches to C_{F2} while the flow velocity remains at u_0. The governing equation to describe the column dynamics is

$$\rho \frac{\partial q}{\partial t} + \varepsilon \frac{\partial C}{\partial t} + u_0 \varepsilon \frac{\partial C}{\partial Z} = 0 \tag{1}$$

where C is the dye concentration in the mobile phase, q is the dye concentration in the stationary phase, ρ is the carbon bed density, ε is the void fraction of the bed, u_0 is the linear velocity of the carrier fluid, t is the operating time, and Z is the distance from the inlet of the mobile phase. The initial condition for Eq. (1) is

$$\text{At } t = 0, \qquad C = C_P \qquad \text{and} \qquad q = q_P$$

The boundary condition for Eq. (1) is

$$\begin{aligned} \text{At } Z = 0, \qquad & C = C_{F1} \quad \text{and} \quad q = q_{F1} \quad \text{for} \quad 0 < t < t_0 \\ & C = C_{F2} \quad \text{and} \quad q = q_{F2} \quad \text{for} \quad t \geq t_0 \end{aligned}$$

The assumptions associated with Eq. (1) are:

(1) The adsorption reaches local equilibrium.
(2) No chemical reactions occur in the column.
(3) Only mass transfer by convection is significant.
(4) Radial and axial dispersions are negligible.
(5) The flow pattern is ideal plug flow.
(6) The temperature in the column is uniform and invariant with time.
(7) The flow rate is constant and invariant with the column position.

The dye concentration in the stationary phase is related to that in the mobile phase by the Redlich–Peterson adsorption isotherm model (21):

$$q = \frac{AC}{B + C^M} \tag{2}$$

MARCEL DEKKER, INC.
270 Madison Avenue, New York, New York 10016

Although Eqs. (1) and (2) associated with the initial and boundary conditions can be solved for $C = C(Z, t)$ by numerical methods, the cause-and-effect relation between the column dynamics and the feed concentration change cannot be clearly figured out. To illustrate the cause-and-effect relation, simple expressions based on the wave interference theory will be developed. Depending upon the relative magnitude of C_P, C_{F1}, and C_{F2}, there are six different wave interference cases as shown in Fig. 1, but only two of them will be considered in this paper.

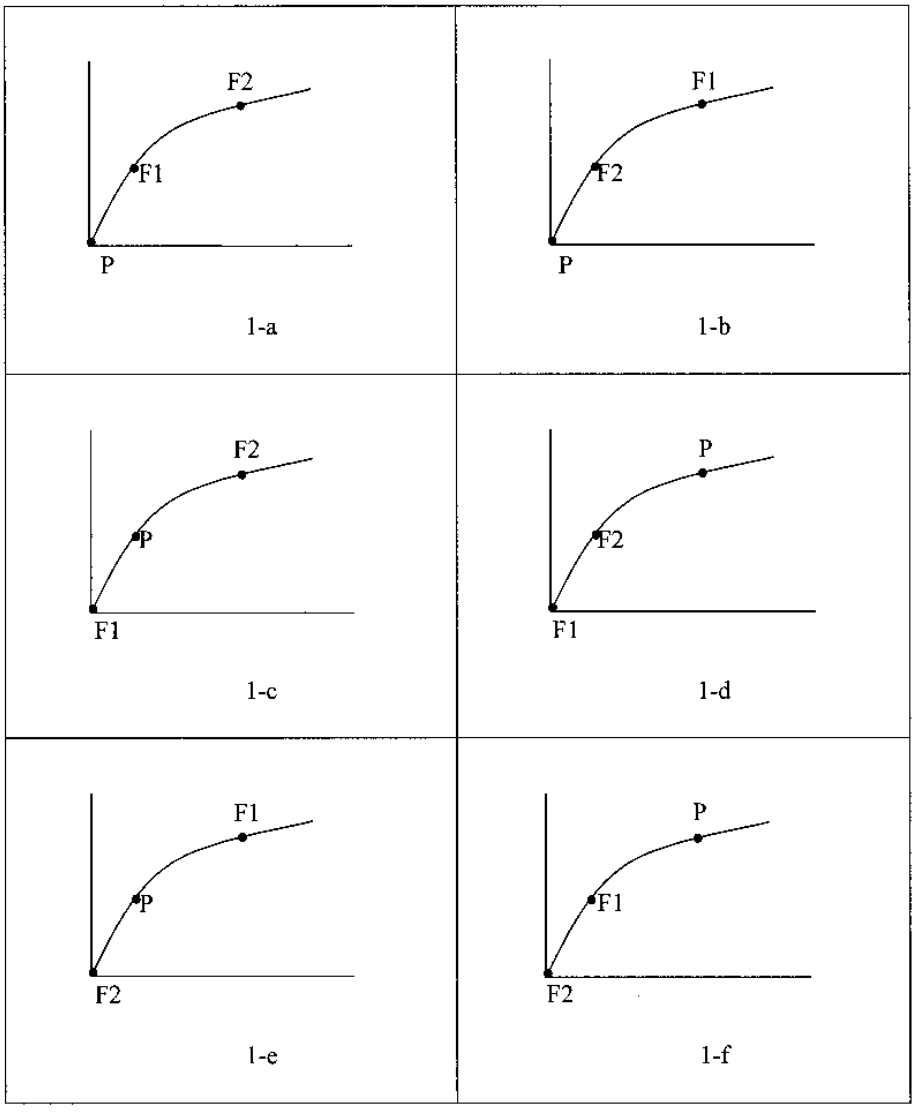

FIG. 1 Six different wave interference cases.

MARCEL DEKKER, INC.
270 Madison Avenue, New York, New York 10016

Case 1. $C_P < C_{F1} < C_{F2}$

According to the wave propagation theory (1, 7), the introduction of the first feed results in a self-sharpening wave with the wave velocity

$$u_{F1\to P} = \frac{u_0}{1 + \frac{\rho}{\varepsilon}\left(\frac{q_{F1} - q_P}{C_{F1} - C_P}\right)} \tag{3}$$

This concentration wave velocity is the slope of the straight line originating at $t = 0$ and separating concentration P from F1 in the distance–time (Z–t) diagram as is shown schematically in Fig. 2-a. The switch to the second feed concentration at $t = t_0$ also results in a self-sharpening wave with the wave velocity

$$u_{F2\to F1} = \frac{u_0}{1 + \frac{\rho}{\varepsilon}\left(\frac{q_{F2} - q_{F1}}{C_{F2} - C_{F1}}\right)} \tag{4}$$

This concentration wave velocity is the slope of the straight line originating at $t = t_0$ and separating concentration F1 from F2 in the Z–t diagram as is also shown schematically in Fig. 2-a. One can easily see from Fig. 2-b that

$$\frac{q_{F2} - q_{F1}}{C_{F2} - C_{F1}} < \frac{q_{F1} - q_P}{C_{F1} - C_P}$$

Therefore,

$$u_{F2\to F1} > u_{F1\to P}$$

Because the second feed concentration wave is faster than the first one, it will catch the first feed concentration wave at $t = t_1$, which can be obtained from solving the following equations simultaneously:

$$\begin{cases} Z_1 = u_{F1\to P} t_1 \\ Z_1 = u_{F2\to F1}(t_1 - t_0) \end{cases} \tag{5}$$

Thus,

$$t_1 = \frac{u_{F2\to F1}}{u_{F2\to F1} - u_{F1\to P}} t_0 \tag{6}$$

The corresponding position at which two waves meet each other is

$$Z_1 = \frac{u_{F2\to F1} u_{F1\to P}}{u_{F2\to F1} - u_{F1\to P}} t_0 \tag{7}$$

Once the second feed concentration wave catches the first one, wave interfer-

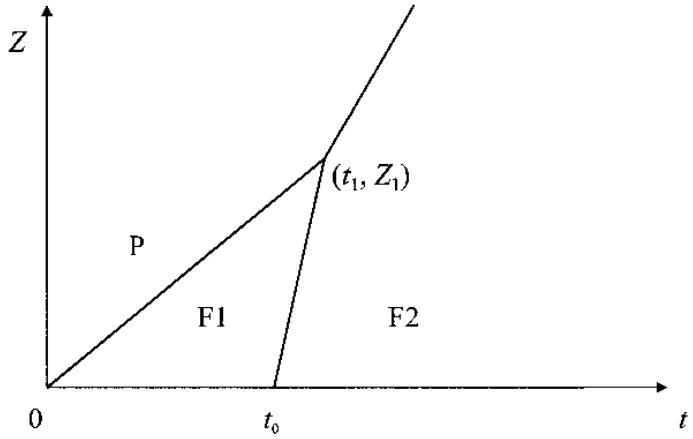

2-a

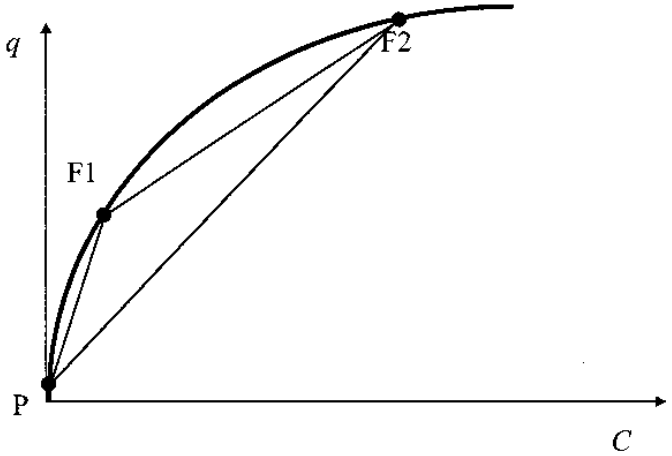

2-b

FIG. 2 Schematic diagrams showing wave interference for $C_P < C_{F1} < C_{F2}$. 2-a: Distance–time diagram. 2-b: Adsorption isotherm.

ence phenomenon occurs and results in a self-sharpening wave with the wave velocity

$$u_{F2\to P} = \frac{u_0}{1 + \frac{\rho}{\varepsilon}\left(\frac{q_{F2} - q_P}{C_{F2} - C_P}\right)} \tag{8}$$

This concentration wave velocity is the slope of the straight line originating at the point $t = t_1$, $Z = Z_1$, and separating composition F2 from P in the Z–t diagram as is shown schematically in Fig. 2-a. As shown in Fig. 2-b,

$$\frac{q_{F2} - q_{F1}}{C_{F2} - C_{F1}} < \frac{q_{F2} - q_P}{C_{F2} - C_P} < \frac{q_{F1} - q_P}{C_{F1} - C_P}$$

Therefore,

$$u_{F2\to F1} > u_{F2\to P} > u_{F1\to P}$$

This suggests that the first slow P|F1 cut wave will be accelerated, the second fast F1|F2 cut wave will be slowed down, and the waves will merge into a P|F2 cut wave with velocity in between the two waves.

The effluent history can be easily obtained by plotting a horizontal line $Z = L$ in the Z–t diagram as is shown in Fig. 3. Depending upon the bed length, L, the effluent history or the so-called breakthrough curve may have different shapes. Figure 3-a shows the case for $L < Z_1$. In this case the bed length is shorter than the position where wave interference occurs; the first feed concentration wave leaves the bed before it can be caught by the second one. There are therefore two breakthrough times, one for the first feed concentration and the other for the second. Figure 3-b shows the case for $L > Z_1$. In this case the bed length is longer than the position where wave interference occurs; the first feed concentration wave is caught and merged by the second one. There is therefore only one breakthrough time for the second feed concentration.

Case 2. $C_P < C_{F2} < C_{F1}$

In this case the introduction of the first feed also results in a self-sharpening wave with the wave velocity calculated by Eq. (3). This concentration

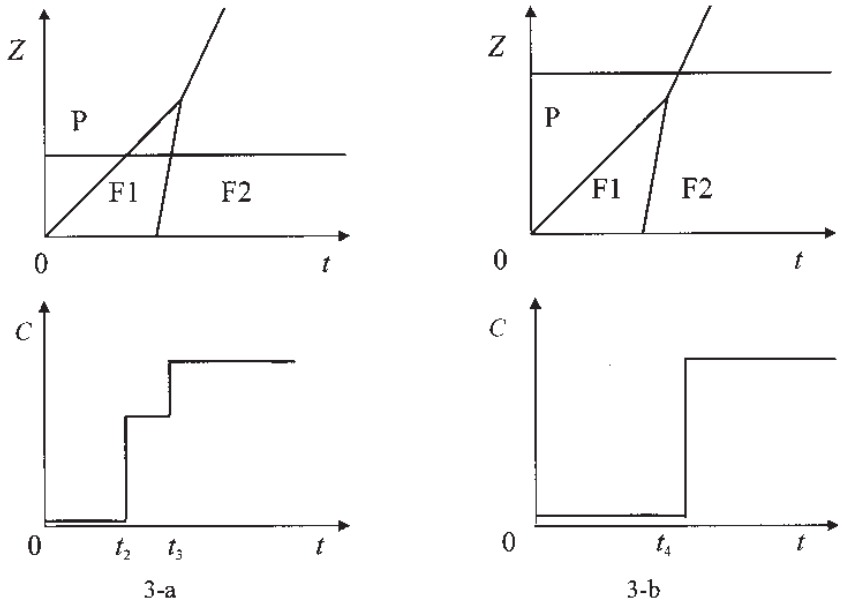

FIG. 3 Schematic diagrams showing wave interference for $C_P < C_{F1} < C_{F2}$. 3-a: $L < Z_1$. 3-b: $L > Z_1$.

wave velocity is the slope of the straight line originating at $t = 0$ and separating concentration P from F1 in the Z–t diagram as is shown schematically in Fig. 4-a. The switch to the second feed concentration at $t = t_0$ results in a non-sharpening wave with the wave velocity

$$u_C = \frac{u_0}{1 + \frac{\rho}{\varepsilon}\left(\frac{dq}{dC}\right)}, \qquad \text{for } C_{F2} \le C \le C_{F1} \tag{9}$$

The concentration wave velocities are the slopes of the straight lines all originating at $t = t_0$ and separating concentration F1 from F2 in the Z–t diagram as is shown schematically in Fig. 4-a. Theoretically, there are infinite numbers

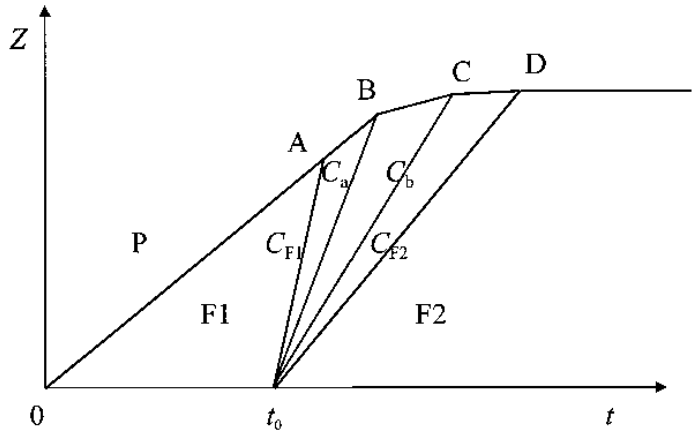

4-a

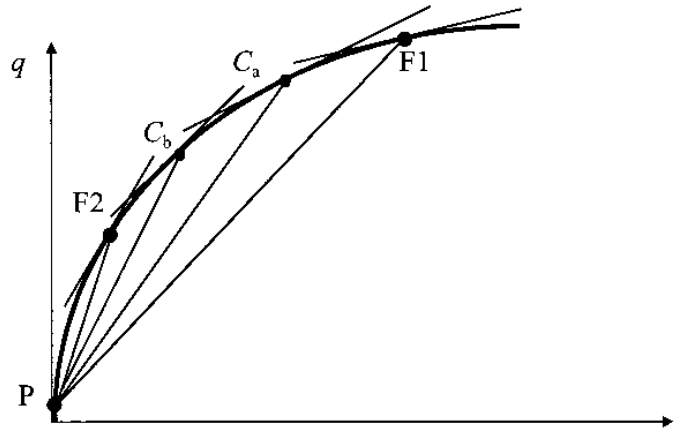

4-b

FIG. 4 Schematic diagrams showing wave interference for $C_P < C_{F2} < C_{F1}$. 4-a: Distance–time diagram. 4-b: Adsorption isotherm.

MARCEL DEKKER, INC.
270 Madison Avenue, New York, New York 10016

of straight lines representing the continuous variation of the concentration from the first feed to the second. Shown in Fig. 4-a are only four lines to illustrate the procedure to obtain the Z–t curve after wave interference occurs.

As shown in Fig. 4-b, the nonsharpening F1|F2 cut wave velocity of the first feed concentration is greater than the self-sharpening P|F1 cut wave velocity of the first feed concentration because the tangent slope at F1 is less than the chord slope of $\overline{\text{F1P}}$. Therefore, the nonsharpening F1|F2 cut wave will catch the self-sharpening P|F1 cut wave and this results in another self-sharpening wave, separating the presaturation concentration P from the first feed concentration F1. As is shown in Fig. 4-b, the nonsharpening wave velocity of concentration C_a is greater than the self-sharpening P|F1 cut wave velocity because the tangent slope at C_a is less than the chord slope of $\overline{\text{F1P}}$. Therefore the self-sharpening P|F1 cut wave will be caught by the nonsharpening wave of concentration C_a and this results in another self-sharpening P|C_a cut wave.

As in Case 1, the first wave interference Point A, shown in Fig. 4-a, locates at $t = t_A$ and $Z = Z_A$, which can be calculated by Eqs. (6) and (7), respectively. The second wave interference Point B locates at $t = t_B$ and $Z = Z_B$, which can be obtained from solving the following simultaneous equations:

$$\begin{cases} Z_B = u_{F1\to P} t_B \\ Z_B = u_{C_a}(t_B - t_0) \end{cases} \tag{10}$$

Thus,

$$\begin{cases} t_B = \dfrac{u_{C_a}}{u_{C_a} - u_{F1\to P} t_0} \\ Z_B = \dfrac{u_{C_a} u_{F1\to P}}{u_{C_a} - u_{F1\to P}} t_0 \end{cases} \tag{11}$$

In Eq. (11) the nonsharpening wave for the concentration C_a is calculated by the following equation:

$$u_{C_a} = \frac{u_0}{1 + \dfrac{\rho}{\varepsilon}\left(\dfrac{dq}{dC}\right)} \tag{12}$$

So far, the first two interference points, A and B, are determined and the line segment $\overline{\text{AB}}$ representing the P|F1 cut can be plotted. Similarly, other interference points such as C and D can be determined by the same procedure and the line segments $\overline{\text{BC}}$ and $\overline{\text{CD}}$ representing the P|C_a and P|C_b cuts, respectively, can be obtained.

Once the whole Z–t diagram is obtained, the effluent history can be easily obtained by plotting a horizontal line $Z = L$ in the Z–t diagram as is shown in Fig. 5. Again, depending upon the bed length, L, the effluent history may have

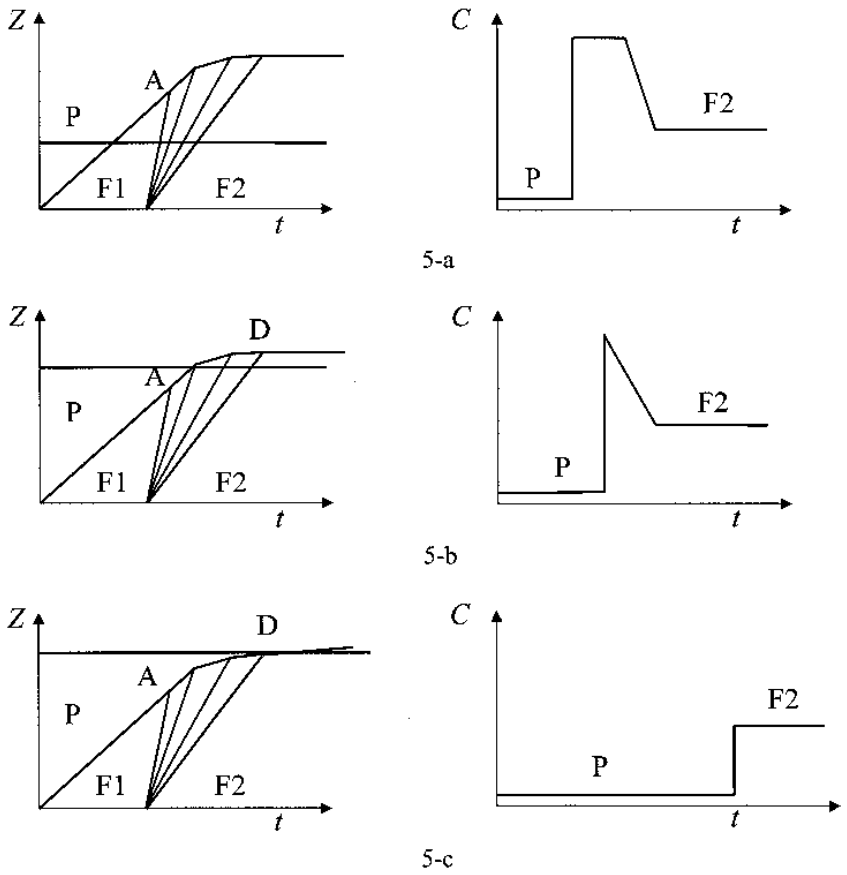

FIG. 5 Schematic diagrams showing wave interference for $C_P < C_{F1} < C_{F2}$. 5-a: $L < Z_A$. 5-b: $Z_A < L < Z_D$. 5-c: $L > Z_D$.

different shapes. Figure 5-a shows the case for $L < Z_A$. In this case the bed length is shorter than the position where the first wave interference point occurs; the first feed concentration wave leaves the bed before it can be caught by the second one. Therefore, at the first breakthrough time, the effluent concentration jumps from the presaturation concentration to the first feed concentration. Then the effluent concentration remains at the first feed concentration for a while until the first feed concentration wave is caught by the second feed one. Once the second feed concentration wave catches the first one, wave interference phenomenon occurs and makes the effluent concentration decrease from the first feed one to the second feed one. Finally, the second feed concentration breaks through and the effluent concentration remains at that concentration.

Figure 5-b shows the case for $Z_A < L < Z_D$. In this case the effluent concentration jumps from the presaturation concentration to a concentration in between the first feed one and the second feed one, and then decreases to the

second feed concentration. Finally, the second feed concentration will also break through.

Figure 5-c shows the case for $L > Z_D$. In this case the bed is so long that the first feed concentration wave is totally run over by the second one, therefore the effluent concentration jumps from the presaturation concentration to the second feed one and then remains at that concentration.

EXPERIMENTAL

Yellow acid dye (Sumitomo Chemical Corp., Japan) with the main ingredient triphenyalmethane was used to prepare the synthetic wastewater for the column tests in this study. Granular activated carbon (Taipei Chemical Corp., Taiwan) with a size range between 30 and 32 mesh was used. The column tests were carried out in a water-jacketed glass column with an inside diameter of 1.20 cm. A fixed volume of the yellow dye solution was fed to the top of the column by a metering pump (Watson-Marlow, 302S/RL), flowed through the carbon bed, and then exited from the bottom of the column. After the fixed volume of the dye solution flowed through the bed, a second feed with a different dye concentration was introduced to the column. Other experimental details can be found in the previous paper (21). The presaturation and feed compositions of the column tests are summarized in Table 1.

RESULTS AND DISCUSSION

The adsorption isotherm of the yellow dye at 25°C was determined in the previous study (21) and was best represented by the Redlich–Peterson model with the parameters shown in Table 2. Using these parameters and the equations developed above, the effluent concentrations for all the column test runs can be predicted.

In practice, one can plot the in-bed volume versus cumulative effluent volume diagram with the slope being the dimensionless concentration wave velocity, $1/[\varepsilon + \rho(dq/dC)]$ or $1/[\varepsilon + \rho(\Delta q/\Delta C)]$, to replace the distance–time

TABLE 1
Presaturation and Feed Composition of Column Tests

	Run 1	Run 2	Run 3	Run 4
Presaturation concentration (mg/L)	0	0	0	0
First feed concentration (mg/L)	200	200	492	492
Volume of first feed (L)	3.5	3.5	1.5	1.2
Second feed concentration (mg/L)	486	486	20	20

TABLE 2
Redlich–Peterson Adsorption Model Parameters for the Yellow Dye at 25°C

Parameter	Value	Unit
A	842	$mg/g/(mg/L)^{0.087}$
B	0.266	$(mg/L)^{0.913}$
M	0.913	—

diagram with the slope being the concentration wave velocity. The in-bed volume is the volume traveled by the concentration wave. The feed-switch time t_0 is correspondingly replaced by the total volume of the first feed flowing through the column.

The $V_{\text{in-bed}}$ vs V_{eff} diagram for Run 1 is shown in Fig. 6 with the interference point being $V_{\text{eff}} = 3375$ BV and $V_{\text{in-bed}} = 1.6$ BV. Since the interference in-bed volume is greater than unity, the first feed concentration will break through before it is caught by the second one. There are therefore two breakthrough volumes, one for the first feed concentration and the other for the second, as shown in Fig. 6. The experimental and predicted

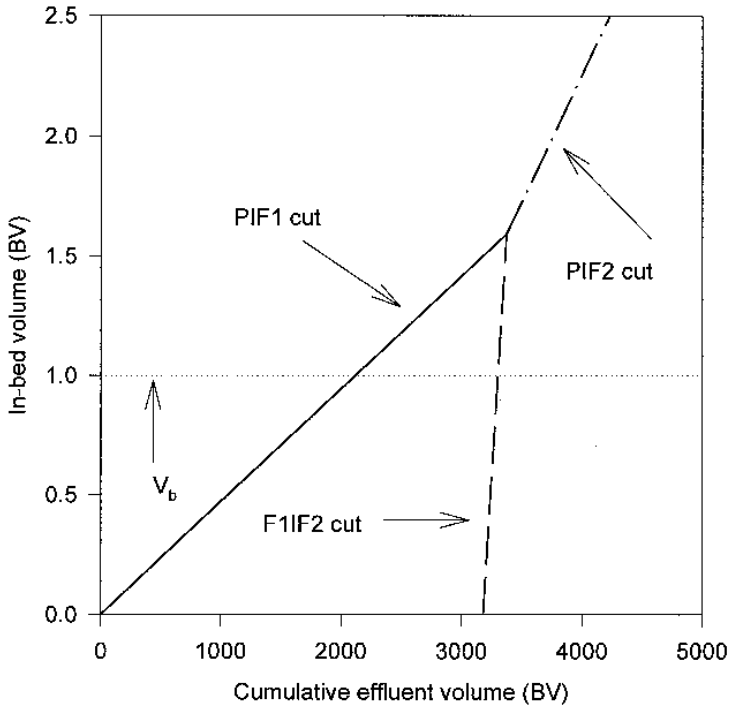

FIG. 6 In-bed volume versus cumulative effluent volume diagram for column test Run 1.

breakthrough curves for Run 1 are shown in Fig. 7. As one can see from Fig. 7, the wave interference theory gives satisfactory prediction of the breakthrough curve.

The $V_{\text{in-bed}}$ vs V_{eff} diagram for Run 2 is shown in Fig. 8 with the interference point being $V_{\text{eff}} = 1954$ BV and $V_{\text{in-bed}} = 0.9$ BV. Since the interference in-bed volume is less than unity, the first feed concentration will be caught and merged by the second one. There is therefore only one breakthrough volume for the second feed concentration, as shown in Fig. 8. The experimental and predicted breakthrough curves for Run 2 are shown in Fig. 9. As one can see from Fig. 9, the wave interference theory also gives quite satisfactory prediction of the breakthrough curve.

The $V_{\text{in-bed}}$ vs V_{eff} diagram for Run 3 is shown in Fig. 10 with the first interference point being $V_{\text{eff}} = 1265$ BV and $V_{\text{in-bed}} = 1.35$ BV. Since the interference in-bed volume is greater than unity, the first feed concentration will break through before it is caught by the second one. This wave interference phenomenon results in the breakthrough curve shown in Fig. 11. The $V_{\text{in-bed}}$ vs V_{eff} diagram for Run 4 is shown in Fig. 12 with the first interference point being $V_{\text{eff}} = 940$ BV and $V_{\text{in-bed}} = 1$ BV. In this run, as soon as the first feed concentration leaves the column, the wave interference phenomenon occurs. The resulting breakthrough curves are shown in Fig. 13.

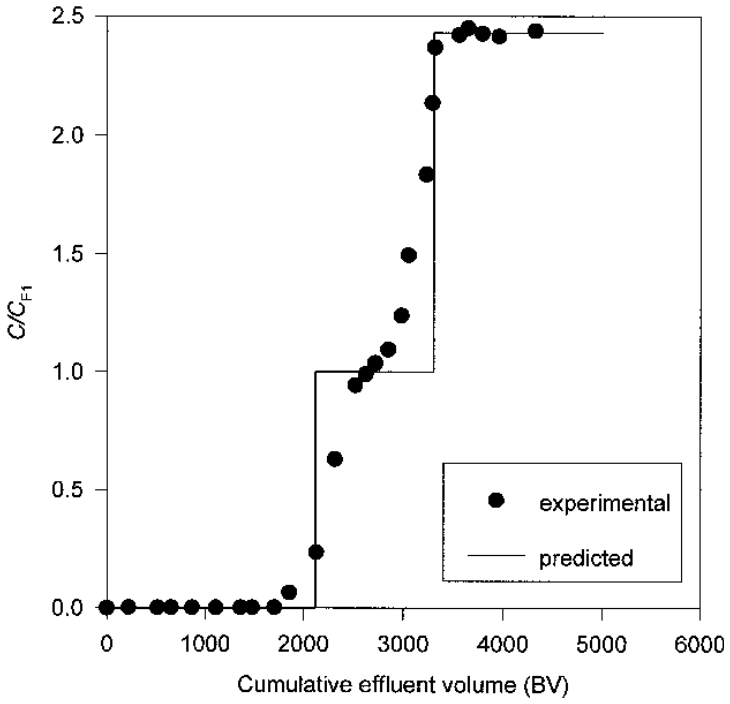

FIG. 7 Breakthrough curve for column test Run 1.

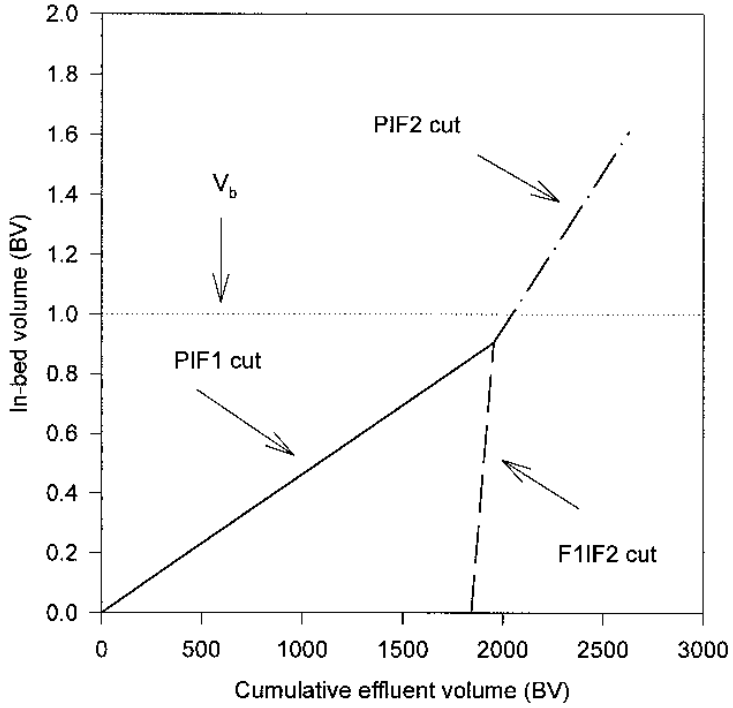

FIG. 8 In-bed volume versus cumulative effluent volume diagram for column test Run 2.

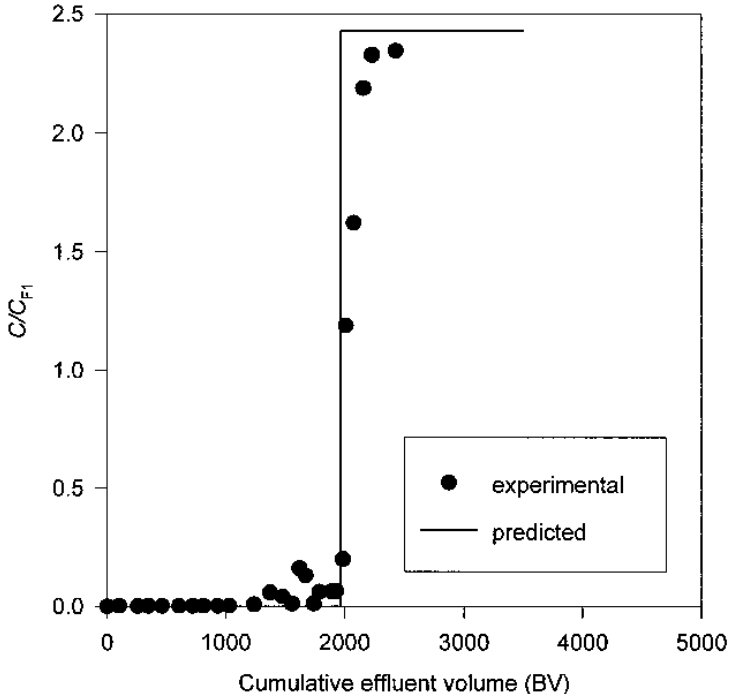

FIG. 9 Breakthrough curve for column test Run 2.

MARCEL DEKKER, INC.
270 Madison Avenue, New York, New York 10016

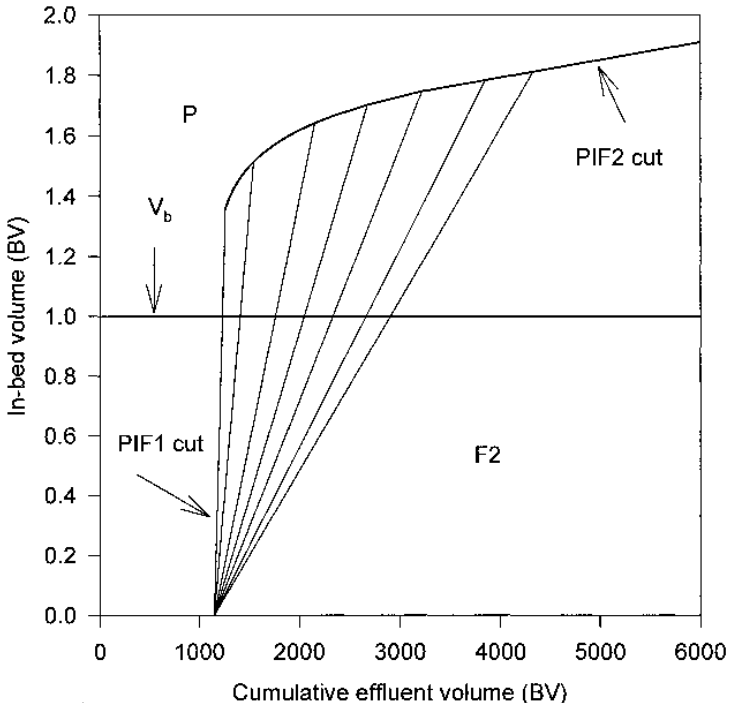

FIG. 10 In-bed volume versus cumulative effluent volume diagram for column test Run 3.

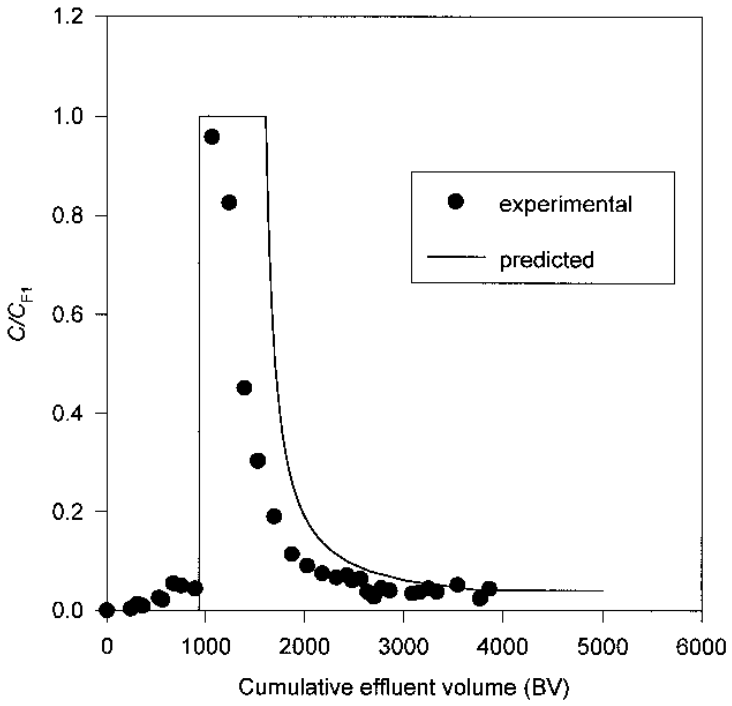

FIG. 11 Breakthrough curve for column test Run 3.

MARCEL DEKKER, INC.
270 Madison Avenue, New York, New York 10016

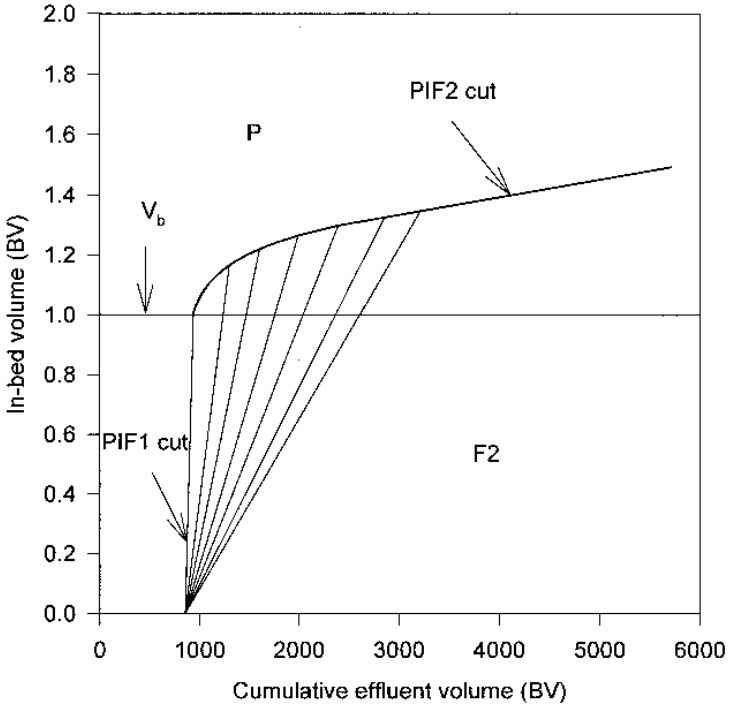

FIG. 12 In-bed volume versus cumulative effluent volume diagram for column test Run 4.

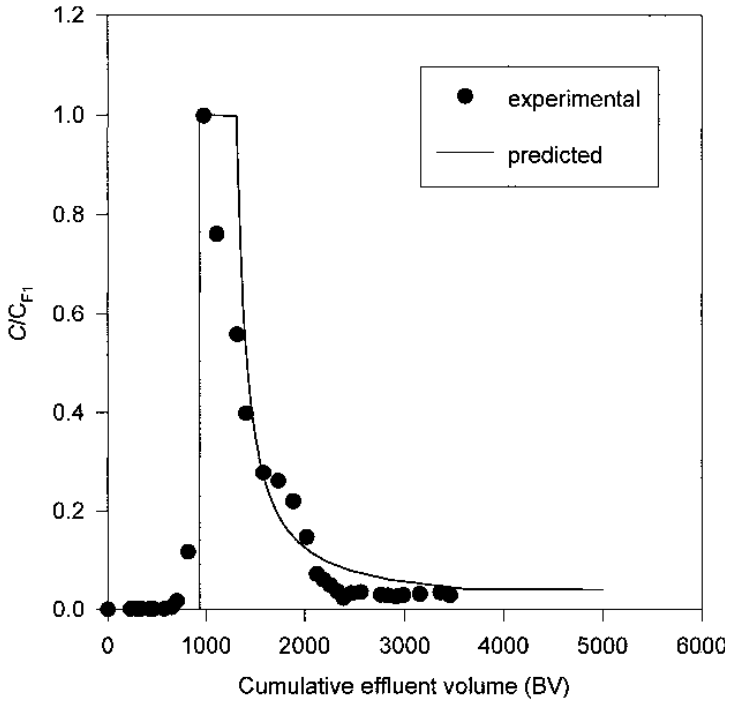

FIG. 13 Breakthrough curve for column test Run 4.

MARCEL DEKKER, INC.
270 Madison Avenue, New York, New York 10016

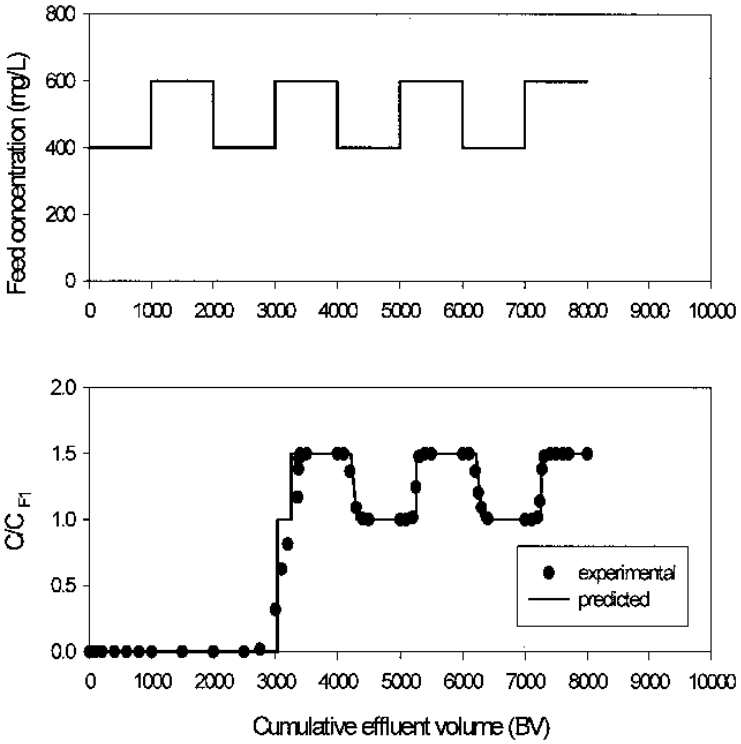

FIG. 14 Breakthrough curve for column test run with cyclic feed concentration change.

In addition to the above four test runs whose breakthrough curves can be satisfactorily predicted by the wave interference theory, another column test run with a cyclic feed concentration change was performed to further validate the applicability of the theory. The column was initially packed with fresh activated carbon, and the 400- and 600-mg/L yellow dye solutions were cyclically fed to the column. The feed concentration and the breakthrough curve for this test run are shown in Fig. 14. The wave interference phenomenon of this test run contains the two interference cases discussed above; both self-sharpening and nonsharpening waves result from feed concentration interference. Again the wave interference theory predicts the breakthrough curve satisfactorily.

CONCLUSIONS

The effluent histories of yellow dye adsorption by an activated carbon bed are experimentally measured and theoretically predicted by the wave interference theory. Explicit expressions have been developed from the wave interference theory to predict the single-component adsorption column dynamics with the feed concentration change. Five column tests of yellow dye adsorp-

tion by an activated carbon bed are performed, and the results show that the dye effluent histories predicted by the wave interference theory are in good agreement with the experimental ones.

This study provides a handy methodology to understand the cause-and-effect relations of wave interference phenomena. Without solving the governing equation for the column dynamics, the theory uses the concept of wave propagation and simple calculations to construct the distance–time diagram. Then the effluent histories can be easily obtained if the bed length is specified.

NOMENCLATURE

A	Redlich–Peterson model constant [kg/kg-$(kg/m^3)^{1-M}$]
B	Redlich–Peterson model constant [$(kg/m^3)^M$]
C	dye concentration in mobile phase (kg/m^3)
C_P	presaturation dye concentration in mobile phase (kg/m^3)
C_{F1}	first-feed dye concentration in mobile phase (kg/m^3)
C_{F2}	second-feed dye concentration in mobile phase (kg/m^3)
M	Redlich–Peterson model constant
q	dye concentration in stationary phase (kg/kg carbon)
q_P	presaturation dye concentration in stationary phase (kg/kg carbon)
q_{F1}	dye concentration in stationary phase equilibrium with first feed (kg/kg carbon)
q_{F2}	dye concentration in stationary phase equilibrium with second feed (kg/kg carbon)
t	time (h)
u_0	linear velocity of carrier fluid (m/h)
$u_{F1\rightarrow P}$	concentration wave velocity of F1|P cut (m/h)
$u_{F2\rightarrow F1}$	concentration wave velocity of F2|F1 cut (m/h)
Z	distance from the inlet of mobile phase (m)
ε	void fraction of bed
ρ	carbon bed density (kg/m^3)

ACKNOWLEDGMENT

This work was supported by the National Science Council of Taiwan, Republic of China (Grant NSC85-2211-E-036-001).

REFERENCES

1. F. G. Helfferich and G. Klein, *Multicomponent Chromatography*: *Theory of Interference*, Dekker, New York, NY, 1970.
2. F. G. Helfferich, "Wave Propagation: The Coherence Principle—An Introduction," in *Migration and Fate of Pollutants in Soil and Subsoils* (D. Petruzzeli and F. G. Helfferich,

Eds.; NATO Advanced Study Institute Series G32), Springer-Verlag, Berlin, Germany, 1993.
3. I. M. Klotz, "The Adsorption Wave," *Chem. Rev.*, *39*, 241 (1946).
4. E. Glueckauf and J. I. Coates, "Theory of Chromatography, Part IV: The Influence of Incomplete Equilibrium on the Front Boundary of Chromatograms and on the Effectiveness of Separation," *J. Chem. Soc. (London)*, p. 1315 (1947).
5. F. G. Helfferich, "Multicomponent Ion Exchange in Fixed Beds: Generalized Equilibrium Theory for Systems with Constant Separation Factors," *Ind. Eng. Chem., Fundam., 6*, 362 (1967).
6. F. G. Helfferich, "Chromatographic Behavior of Interfering Solutes: Conceptual Basis and Outline of a General Theory," *Adv. Chem. Ser., 79*, 30 (1968).
7. F. G. Helfferich and P. W. Carr, "Non-linear Waves in Chromatography: I. Waves, Shocks, and Shapes," *J. Chromatogr., 629*, 97 (1993).
8. Y.-L. Hwang, "Wave Propagation in Mass-Transfer Processes: From Chromatography to Distillation," *Ind. Eng. Chem. Res., 34*, 2849 (1995).
9. G. McKay, "Adsorption of Dyestuffs from Aqueous Solution Using Activated Carbon: Analytical Solution for Batch Adsorption Based on External Mass Transfer and Pore Diffusion," *Chem. Eng. J., 27*, 187 (1983).
10. G. McKay, M. S. Otterburn, and J. A. Aga, "Fuller's Earth and Fired Clay as Adsorbents for Dyestuffs—Equilibrium and Rate Studies," *Water Air Soil Pollut., 24*, 307 (1985).
11. G. S. Gupta, G. Prasad, K. K. Panday, and V. N. Singh, "Removal of Chrome Dye from Aqueous Solutions by Fly Ash," *Ibid., 37*, 13 (1988).
12. V. Meyer, F. H. H. Carlsson, and R. A. Oellermann, "Decolourization of Textile Effluent Using a Low Cost Natural Adsorbent Material," *Water Sci. Technol., 26*, 1205 (1992).
13. H. Yoshida, A. Okamoto, and T. Kataoka, "Adsorption of Acid Dye on Cross-Linked Chitosan Fibers: Equilibria," *Chem. Eng. Sci., 48*, 2267 (1993).
14. C. Namasivayam, R. Jeyakumar, and R. T. Yamuna, "Dye Removal from Wastewater by Adsorption on 'Waste' Fe(III)/Cr(III) Hydroxide," *Waste Manage., 14*, 643 (1994).
15. N. E. Krupa and F. S. Cannon, "GAC: Pore Structure versus Dye Adsorption," *J. Am. Water Works Assoc., 88*, 94 (1996).
16. N. Deo and M. Ali, "Dye Removal from Aqueous Solutions by Adsorption on a Low Cost Material," *J. Inst. Eng. (India): Environ. Eng. Div., 76*, 48 (1996).
17. R.-S. Juang and S.-L. Swei, "Effect of Dye Nature on Its Adsorption from Aqueous Solution onto Activated Carbon," *Sep. Sci. Technol., 31*, 2143 (1996).
18. T. Vermeulen, D. LeVan, N. K. Hiester, and G. Klein, "Adsorption and Ion Exchange," in *Perry's Chemical Engineers' Handbook*, 6th ed. (R. H. Perry, D. W. Green, and J. O. Maloney, Eds.), McGraw-Hill, New York, NY, 1984.
19. D. M. Ruthven, *Principles of Adsorption and Adsorption Processes*, Wiley, New York, NY, 1984.
20. F. G. Helfferich and R. D. Whitley, "Non-linear Waves in Chromatography: II. Wave Interference and Coherence in Multicomponent Systems," *J. Chromatogr. A, 734*, 7 (1996).
21. J.-M. Chern and S.-N. Huang, "Study of Non-linear Wave Propagation Theory: 1. Dye Adsorption by Activated Carbon," *Ind. Eng. Chem. Res., 37*, 253 (1998).

Received by editor July 29, 1998
Revision received November 1998

PAGE 2012 IS BLANK

MARCEL DEKKER, INC.
270 Madison Avenue, New York, New York 10016

Request Permission or Order Reprints Instantly!